



Exploratory Design and Evaluation of Alumina-Based Oxide/Oxide Ceramic Matrix Composite for Integrated Thermal Protection System Application

Vinh Tung Le¹ and Abhendra K. Singh²

Abstract

In this study, fabrication and testing of an integrated thermal protection system (TPS) based on alumina-based Oxide/Oxide ceramic matrix composite is performed. The structure is based on an open-channel core sandwich concept and is fabricated using prepregs that constitute Nextel™720 fiber and alumina matrix. Fabricated sandwich panels are tested for survivability, extent of physical degradation, and overall thermal resilience by being subjected to inductively generated air plasma in near-vacuum environment that simulates high altitude hypersonic flight condition. In addition, one-sided thermal shock and hold tests are performed using a furnace at multiple temperatures and durations in order to evaluate pure thermal effects on the structure. Micro-CT scans are used to assess the microstructure of the sandwich composite both before and after the individual thermal tests. The flexural response and impact damage resistance of the sandwich structure are also evaluated at room temperature. The thermal and structural test results combined provide useful information regarding the utility of the adopted design, as well as the success of the fabrication method. The study also exposes the limitations of the sandwich composite design that need to be overcome in order to arrive at a robust oxide-based sandwich composite for use as load bearing TPS in hypersonic vehicles.

Keywords: *oxide/oxide, ceramic matrix composite, thermal protection system, sandwich composite*

1. Introduction

One of the key issues in ensuring the safety of a hypersonic reentry flight is to keep the underlying structure within acceptable temperature limits. In this regard, thermal protection system (TPS) is essential to protect the internal structure of the vehicle from overheating that may happen due to the aerodynamic heating on the external structures and simultaneous heat transfer [1]. The major requirement for materials used for TPS applications in reusable vehicles is that they must be able to withstand high temperature. Additionally, they must be lightweight and structurally and environmentally durable at such elevated temperatures. Considering all these attributes, ceramic matrix composites (CMCs) are well positioned to be used for TPS applications. For example, the C/C-SiC CMC has been used for designing a TPS of SHEFEX II hypersonic reentry body, which returned to Earth at Mach 10.2 [2]. The C/C and C/SiC CMCs were also used to create leading edges and control surfaces of X-38 Mach 10 reentry vehicle [3].

Traditional design of a TPS with the primary function of limiting heat transfer into the internal structure may not fulfil the modern hypersonic vehicle design requirements. These traditional designs can compromise the safety of the vehicle, inviting failure due to high thermal gradients, pressure loads and unpredictable events like hypervelocity impacts from space debris [4, 5]. One approach to mitigate these risks is to consider structurally integrated TPS based on sandwich composite technology, which consists of a lightweight cellular core and face sheet. Numerous studies on integrated sandwich structured TPS with various core configurations exist in literature [1]. Among these sandwich structures, open-channel core sandwich structure, which has the advantage of efficient load-bearing capacity and lightweight, has been proposed and studied for integrated TPS [6-8]. In addition to carrying load at

¹ Department of Mechanical Engineering, Baylor University, Waco, TX 76706, USA, tung_le@baylor.edu

² Department of Mechanical Engineering, Baylor University, Waco, TX 76706, USA, abhen_singh@baylor.edu

elevated temperatures, the cellular core can also be filled with insulation that can aid in minimizing heat effects on the rest of the vehicle [6, 9].

Alumina-based Oxide/Oxide CMCs are oxidation resistant and have proven record of carrying mechanical load at elevated temperatures. While the recommended performance temperature of alumina-based Oxide/Oxide CMCs for gas turbine applications is 1200°C [10], this temperature recommendation is based on long durations (many hours) of thermal exposure [11, 12]. The melting point of alumina is 1890°C and the anticipated flight duration for hypersonic vehicles is in minutes. Fig. 1 shows typical flight profiles of a reentry space shuttle [1] and a hypersonic SHEFEX II vehicle [2], where the total time for the reentry of a space shuttle is approximately 30 minutes while the total hypersonic flight time is approximately 10 minutes. This raises the prospect of using alumina-based CMCs for TPS applications for short duration flights at temperatures much higher than 1200°C.

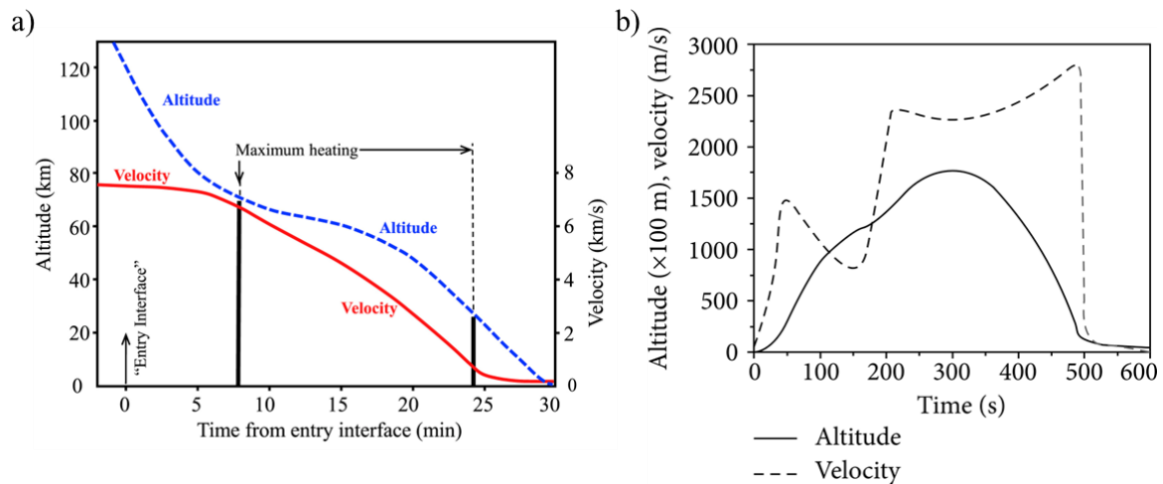


Fig 1. Typical hypersonic flights: a) re-entry profile of a space shuttle [1] and b) hypersonic flight profile of the hypersonic SHEFEX II vehicle [2].

In this study, fabrication and thermal and structural evaluation of integrated TPS composite sandwich structure using alumina-based CMC is explored. Thermal tests are performed to evaluate the survivability, physical degradation and integrity of the face sheet to core bond. Flexural tests are performed for structural evaluation of the sandwich structure, especially the shear load carrying capacity of the core and the strength of the face sheet to core bond. Additionally, impact damage assessment is conducted to analyze the resistance of the sandwich structure to low-velocity impacts and to understand the failure mechanisms under certain impact energies. The overarching goal of this study is to prove concept on the feasibility of using oxide-based CMCs for structurally integrated TPS applications. Additionally, it aims to provide preliminary data regarding the thermal and structural performance of these structures.

2. Material and test methodology

2.1. Material and fabrication

The entire sandwich structure is fabricated using alumina-based AX-7900-720 prepreg acquired from Axiom Materials, Inc., USA. Fig. 2 describes the fabrication process of a CMC based sandwich composite beam. A $[0/90]_{2s}$ layup is used for both the facesheet. Preforms of the two facesheets are hand laid separately, while the open-channel core preform is prepared using a separate steel mold. For the core preform, steel rods with a rectangular cross-section are first prepared with a release spray. The core, with a layup of $[0/90]_s$, is hand laid by wrapping the cut prepregs around steel rods. The required number of core cells are prepared in this manner. The facesheet and core are then placed together, with proper vacuum bagging process, deployed according to the recommendation by the manufacturer. The sandwich structure is then cured pressureless according to manufacturer recommended cycles, followed by sinter in a high temperature air-based furnace. Exactly the same fabrication procedure was used to manufacture sandwich structures of different length and width dimensions, as presented subsequently.

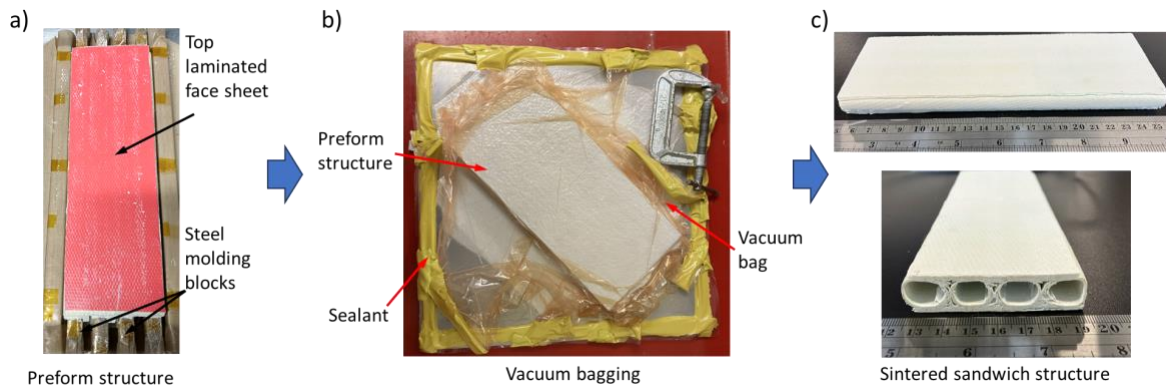


Fig 2. Fabrication process of the open-channel core sandwich composite made of Oxide/Oxide CMCs: a) preform structure, b) vacuum bagging, c) as-fabricated sandwich structure beam after sintering.

2.2 Loading design, requirements, and test matrix

The thermal load chosen in this study is based on the application of the current sandwich structure in a hypersonic vehicle. Fig. 3 shows an example of various materials used in the TPS designs of the Hopper space vehicle, as proposed by the European Space Agency [13, 14]. Here, the designated materials are chosen for specific locations within the vehicle, guided by the maximum temperature at each location. The current sandwich structure is intended for designing TPS with load bearing capability at locations in the hypersonic vehicle where the maximum temperature exceeds 1200°C but is less than the melting point of alumina. These include acreage TPS at windward locations close to the nose cone and hot control surfaces such as elevons and rudders.

The combined effects of thermal exposure temperature and duration is critical to this study for the application for which this structure is proposed. It is well established from extensive research by the gas turbine community that Oxide/Oxide CMCs retain their strength at temperatures below 1200°C for long exposure durations [10, 12]. However, there is a lack of knowledge on degradation kinetics for short exposure durations (in minutes) at temperatures greater than 1200°C but less than the melting point of alumina. Evaluating the thermal response of these structures at such temperatures and durations is one of the prime focuses of this study. These evaluations are performed in both thermal only and thermal plasma environments in this study, the latter motivated by well-established knowledge that in hypersonic flights, there is a dissociation of gas molecules within the boundary layer around the vehicle, resulting in the presence of ionized species in the environment surrounding the vehicle [15]. For the thermal only tests, one sandwich structure was also filled with a high-temperature insulation in the core cavity.

The sandwich structure based integrated TPS is designed to withstand aerodynamic loads, such as pressure typically applied to acreage TPS, as well as drag induced bending moments, shear, and torques commonly experienced by control surfaces [3]. Structures with high strength-to-weight ratio is considered to be a structurally efficient [16]. Additionally, concerning the external surface of hypersonic vehicles, TPS in its lifetime will likely be impacted by low-velocity foreign objects during transportation and integration. Examples of such impacts are dropping of tools or those caused by environmental factors such as hail or runway debris. The sandwich structure based integrated TPS should have sufficient impact damage resistance in order to remain structurally operational. An "obvious" damage of a sandwich structure is defined as damage through the full depth of the sandwich structure [17]. External structures, such as the sandwich-based integrated TPS in this study, shall meet ultimate load requirements and not require immediate repair under an impact energy of approximately 11 Joules (100 in.lb) [17]. Based on these design requirements, the test matrix in Table 1 was developed with

sandwich structures fabricated according to dimensions that were considered suitable for the tests for which they were designated.

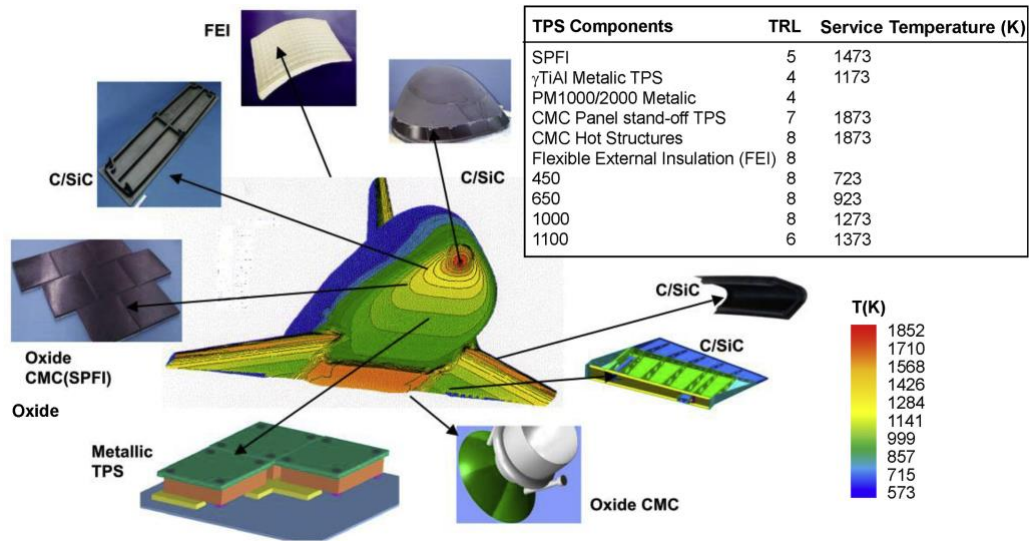


Fig 3. Materials and TPS designs for different locations in the Hopper space vehicle developed by the European Space Agency [1].

Table 1. Test Matrix.

Sample code	Weight (g)	Core length \times Core transverse (mm \times mm)	Average thickness (mm)	Density (g/cm ³)	Designated use
1	41.4	49.4 \times 52.2	15.6	1.03	Furnace test with filled insulation, 1550°C for 30 mins
2	42.3	49.2 \times 50.7	15.5	1.09	Furnace test without filled insulation, 1550°C for 30 mins
3	48.6	50.5 \times 52.7	16.5	1.09	Furnace test without filled insulation, 1200°C for 30 mins
4	52.7	51.0 \times 53.2	16.7	1.16	Furnace test without filled insulation, 1550°C for 10 mins
5	48.3	54.3 \times 48.7	16.3	1.12	Thermal plasma test using inductively generated plasma
6	258.2	208.0 \times 72.6	16.5	1.04	Three-point bend test
7	285.4	152.0 \times 105.0	18.0	0.97	Low-velocity impact test

2.3. Thermal tests

2.3.1 One-sided thermal shock and hold tests

Four different thermal shock and hold tests at different furnace temperatures and exposure durations were performed. Within these, a 1550°C, 30-minute test was done with core filled with alumina-based insulation and another 1550°C, 30-minute test was done without insulation filling. The remaining two tests were done at 1550°C, 10 minutes and 1200°C, 30 minutes. For these tests, a muffle furnace is used to rapidly heat one face sheet of the sandwich structure while keeping the other face sheet exposed to atmosphere. This is done by first bringing the furnace to target test temperature and then exchanging the removeable insulation block at the furnace opening with a grooved block fitted with the

sandwich composite. The sandwich composite was held against the heated furnace chamber for the required test duration. An infrared thermography camera was used to measure the back side temperature of the sandwich structure. Fig. 4 shows the schematic of the furnace test setup. Post-test, the sandwich structures are evaluated for overall survivability as well as other physical changes. X-ray computed tomography was also performed to look for evidence of internal damage. Temperature gradients between the exposed and back sides were assessed in order to understand the effects of test temperature, test duration and inclusion of insulation on possible stresses arising from thermal gradients.

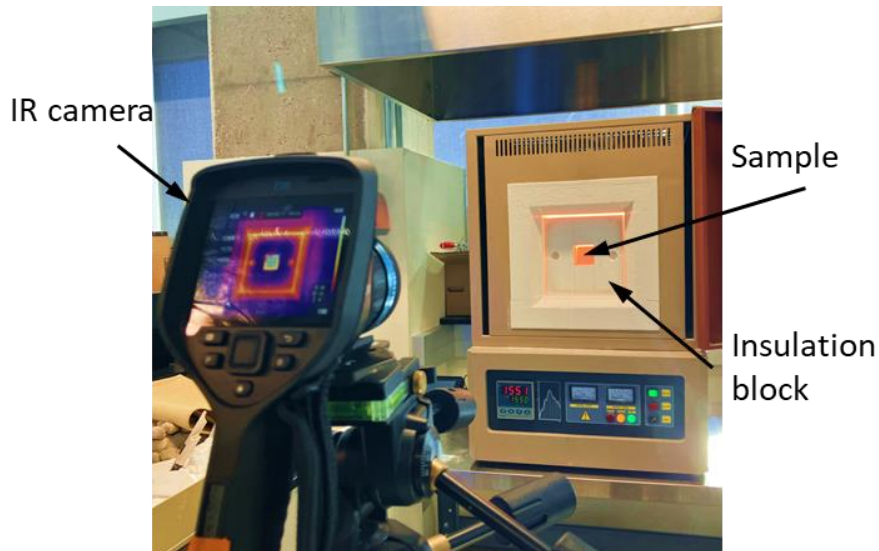


Fig 4. Schematic of the simulated re-entry furnace test setup.

2.3.2 Thermal plasma test using induction plasma generator

The Baylor University induction plasma generator (IPG) has proven capable of performing low-cost, laboratory based thermal-plasma tests on high temperature materials for hypersonic applications [18]. Thermal plasma in this context refers to ultra-high temperature plasma stream that directly impinges the target. Fig. 5 presents a picture of the test setup where a sandwich composite is being exposed to a high temperature plasma stream inside the Baylor University IPG.

Thermal plasma tests are performed in the IPG on the fabricated sandwich structure for up to 30 minutes at a heat flux of $80\text{W}/\text{cm}^2$ using air as the carrier gas. The tests are performed in a closed chamber under near-vacuum conditions, where the chamber pressure in-test is typically around 3 torr. The test was accompanied by critical in-situ diagnostics such as back surface temperature measurement using a Fluke ER1H pyrometer and a Avantes Avaspec 3096 emission spectrometer for identification of emitting species from the target. The temperature read-out range for the pyrometer was 1000°C to 3250°C , i.e., outside of this temperature range the pyrometer could not give an output. A Gardon gage was used to measure the heat flux of the plasma stream prior to placing the target. Post-test, the sandwich structure was evaluated for overall survivability and any evidence of physical degradation or damage.

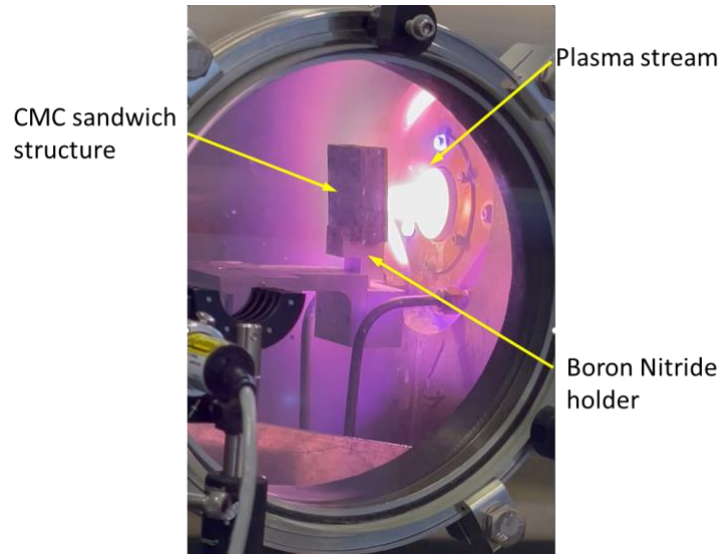


Fig 5. Internal view of the IPG through a quartz window during the plasma test.

2.3. Structural tests

The two structural tests that were performed on the sandwich structure were three-point bend test and low velocity impact test. Sample size for each of these tests is presented in Table 1. One of the reasons for the selection and performance of these tests was to determine the structural integrity of the face sheet to core bond, which is self-formed by the cure and sinter processes. In line with this, the three-point bend test was used to determine the flexural strength of the sandwich composite at room temperature. The test provided critical data on the structural integrity of the sandwich structure and valuable insights into the failure mechanisms, identifying dominant failure modes and related stresses. For the flexural tests, digital image correlation (DIC) was used to get strain data in-test, which were useful in understanding the deformations and failure mechanisms, especially at the face sheet to core bond interfaces. The low-velocity impact test was also carried out at room temperature following ASTM D7766 in order to assess the overall sandwich response and state of damage due to such impact events. The impact energy used for these tests was 11 J. Force, time and displacement results were collected during the test. After the impact test, the state of damage on the impacted side and back side was evaluated.

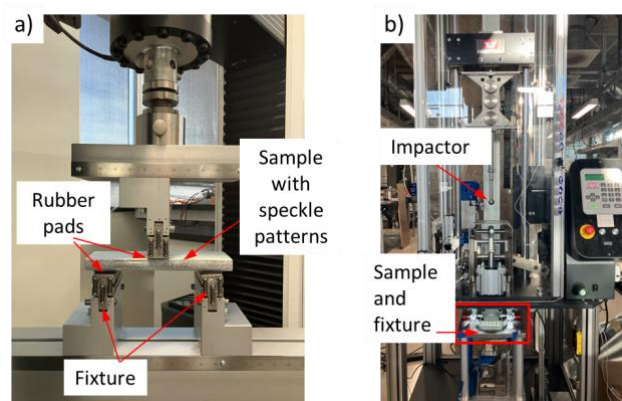


Fig 6. Experimental setup for a) bend test and b) low-velocity impact test

3. Results and discussion

Fig. 7 shows the measured back-side temperature results for the one-sided thermal shock and hold tests performed. In the 1550°C 30-minute tests, the temperature gradient between the exposed and

back side at steady-state was approximately 100°C lower for the case with insulation than the one without it. Also, as expected, the back side rise in temperature to steady-state is slower for the sandwich composite with insulation than the one without it. In comparison to the 1550°C samples, the 1200°C sample showed a slower rise to steady-state temperature, lower back side temperature and smaller temperature gradient between the exposed and back side.

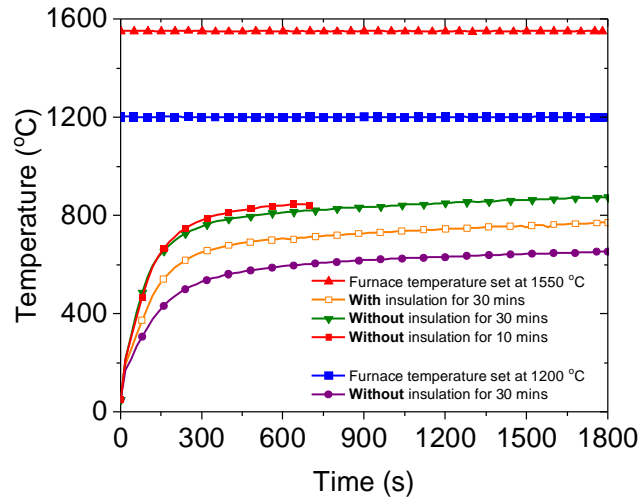


Fig 7. Temperature measurement results for the one-sided thermal shock and hold tests.

No evidence of surface damage was observed in any of the sandwich specimens due to the thermal shock and hold tests. However, for both the 1550°C, 30-minute tests, i.e., with and without insulation, a crack in the top face sheet was observed close to the face sheet to core bond. X-ray CT image showed this cracked region as in-plane and within the top face sheet itself, i.e., it did not extend to or affect the face sheet to core bond. Fig. 8 shows the X-ray CT image of the sandwich composite with insulation after the 1550°C, 30-minute test. Same observations were made for the 1550°C, 30-minute test without insulation. The crack could have been caused by thermal gradient stresses. Further experimental investigation possibly coupled with computational models are needed to correctly establish this. The fact that no such cracking is seen in the 1550°C 10-minute case negates the possibility of thermal shock being the cause of this crack. Rather, it shows exposure duration having an effect on the formation of this crack. In addition, the absence of such crack in the 1200°C case shows exposure temperature also having an effect on the crack formation.

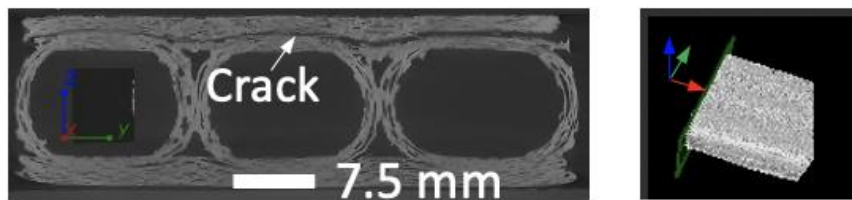


Fig 8. Micro-CT scans of the sandwich structure after thermal test at 1550°C for 30 minutes.

Contrary to the furnace based thermal shock and hold tests, the thermal plasma tests in the IPG showed evidence of damage and other physical changes on the impinged surface of the sandwich structure. The pyrometer could not register a back surface reading, implying that the back surface temperature was less than 1000°C. Also, the emission spectra could not register any evidence of emitting Al or Si from the impingement side. The overall mass change before and after the IPG exposure was negligible. Fig. 9 presents post-test evaluation results of the sandwich composite tested in thermal plasma. There were observable changes in reflectivity of the impinged region in comparison to the rest of the surface (Fig. 9(a)). Several cracks were observed in the impinged region of the face sheet (Fig. 9(b)). It is unclear whether these cracks were due to effects of plasma, or some other effects such as thermal

stresses. This also needs to be investigated further as it is difficult to make conclusions based on just one test result. A small dip was observed in the face sheet right above the location where two adjacent core cells meet. This dip was prevalent in the impinged region and had a measured depth of 100-150 μm (Fig. 9(c)).

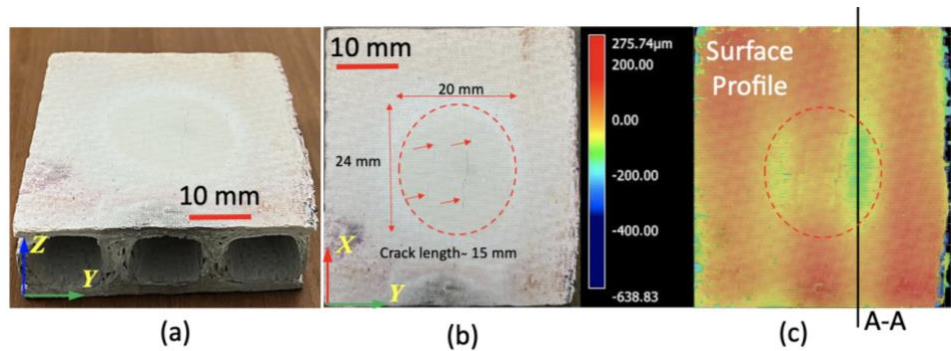


Fig 9. Sandwich structure post thermal plasma test (a) picture, (b) top view and (c) surface profilometry results.

Fig. 10 presents the results of the bend test conducted on a sandwich composite beam. In Fig. 10a, a force versus displacement plot of the test is shown. The observed initial non-linearity in the plot is during the initial loading phase of the test where the fixture fully contacts and settles at the loading points. Following this, there is an observed linear increase in load till crack initiation, where the response becomes non-linear. The first major load drop indicates the failure of the composite beam beyond which its ability to carry further load is significantly compromised. The DIC analysis of major strain revealed that during the transition from linear to nonlinear response, a crack initiated at the bond between the bottom face sheet and the core and propagated. This debond preceded the core shear failure that occurs at the peak load, as illustrated by Fig. 10a. and b. In view of the DIC results, the major loss in structural integrity happens upon core shear. The evaluated specific flexural strength of the composite was $66 \text{ MPag}^{-1}\text{cm}^3$.

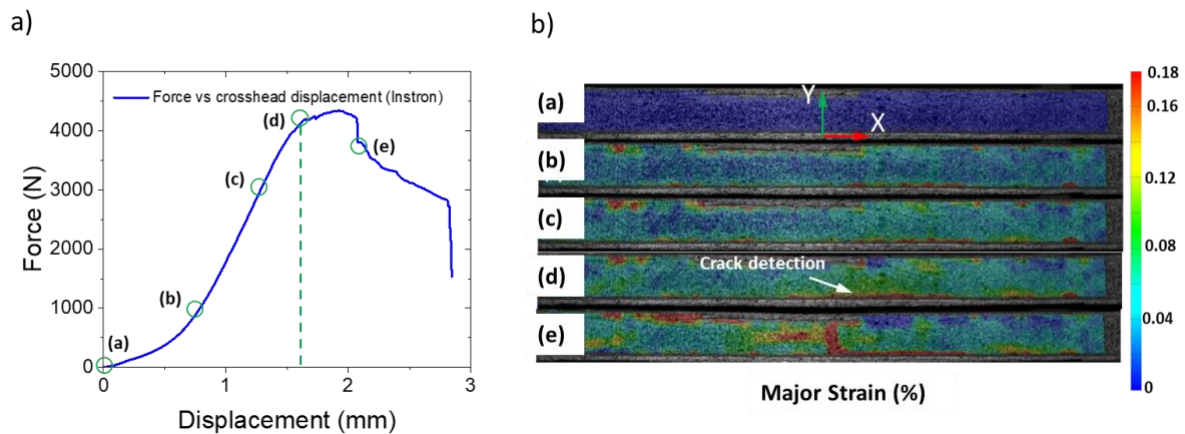


Fig 10. Three-point bend test results: a) load versus displacement and b) DIC major strain.

Fig. 11 illustrates the impact test results of the sandwich composite under an impact energy of 11 J. In Fig. 11a, the load versus displacement curve depicts a rebound action of the impactor, reaching a maximum displacement of approximately 6 mm before rebounding. Fig. 11b presents an inspection of the damage sustained by the sandwich composite. Damage appears localized to the impacted region, with no observed damage to the back face sheet. The maximum evaluated dent depth of the damaged area was 4.2 mm. For the impact energy considered, the localization of top face sheet damage and absence of bottom face sheet damage defied what has been called as "obvious" damage in literature [17].

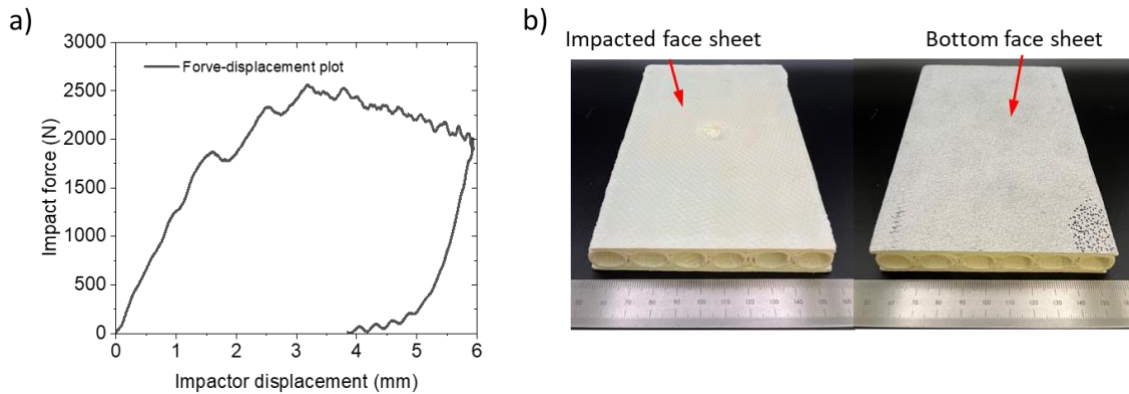


Fig 11. Low velocity impact test result: a) Force versus impactor displacement plot and b) view of top and bottom face sheet.

4. Conclusion

The study presented is exploratory in nature with the results preliminary. However, the concept of sandwich fabrication using Oxide/Oxide CMCs with an open channel core has been successfully demonstrated. Thermal and structural tests were carried out to evaluate the performance of the sandwich composites. All the thermal tests showed the robustness of the face sheet to core bond since failure at bond site was not observed in any instance. However, there is an apparent effect of thermal related stresses that possibly drives failure by face sheet cracking on the exposed side. A specific flexural strength of $66 \text{ MPag}^{-1}\text{cm}^3$ was evaluated, with catastrophic failure happening due to shear failure in the core. While localized face sheet and core damage were observed for an 11 J impact energy on the impacted side, no damage was observed on the bottom face sheet. The results of this study support the prospect of using these structures in hypersonic vehicles. However, additional experimental investigations coupled with thermo-structural computational models are required to fully ascertain this.

References

1. V. T. Le, N. S. Ha, N. S. Goo. Advanced sandwich structures for thermal protection systems in hypersonic vehicles: A review, *Composites Part B: Engineering* Vol. 226, p. 109301, (2021).
2. H. Boehrk, H. Weihs, H. Elsäßer. Hot structure flight data of a faceted atmospheric reentry thermal protection system, *International Journal of Aerospace Engineering* Vol. 2019, pp. 1-16, (2019).
3. D. Glass. "Ceramic Matrix Composite (CMC) Thermal Protection Systems (TPS) and Hot Structures for Hypersonic Vehicles," *15th AIAA International Space Planes and Hypersonic Systems and Technologies Conference*, (2008).
4. N. Knight, K. Song, I. Raju, Space Shuttle Orbiter Wing-Leading-Edge Panel Thermo-Mechanical Analysis for Entry Conditions, *51st AIAA/ASME/ASCE/AHS/ASC Structures, Structural Dynamics, and Materials Conference*, 2010, pp.
5. A. T. Nettles, A. Hodge, J. Jackson, The Effects of Foam Thermal Protection System on the Damage Tolerance Characteristics of Composite Sandwich Structures for Launch Vehicles, 2011.
6. B. Ravishankar, B. Sankar, R. Haftka, Homogenization of integrated thermal protection system with rigid insulation bars, *51st AIAA/ASME/ASCE/AHS/ASC Structures, Structural Dynamics, and Materials Conference 18th AIAA/ASME/AHS Adaptive Structures Conference 12th*, pp. 2687, (2010).
7. A. Sharma, C. Gogu, O. Martinez, B. Sankar, R. Haftka, Multi-fidelity design of an integrated thermal protection system for spacecraft reentry, *49th AIAA/ASME/ASCE/AHS/ASC Structures, Structural Dynamics, and Materials Conference, 16th AIAA/ASME/AHS Adaptive Structures*

- Conference, 10th AIAA Non-Deterministic Approaches Conference, 9th AIAA Gossamer Spacecraft Forum, 4th AIAA Multidisciplinary Design Optimization Specialists Conference, pp. 2062, (2008).
8. Y. Li, L. Zhang, R. He, Y. Ma, K. Zhang, X. Bai, B. Xu, Y. Chen. Integrated thermal protection system based on C/SiC composite corrugated core sandwich plane structure, *Aerospace Science and Technology* Vol. 91, pp. 607-616, (2019).
 9. Y. Xu, N. Xu, W. Zhang, J. Zhu. A multi-layer integrated thermal protection system with C/SiC composite and Ti alloy lattice sandwich, *Composite Structures* Vol. 230, p. 111507, (2019).
 10. K. A. Keller, G. Jefferson, R. J. Kerans. "Oxide–Oxide Composites," *Ceramic Matrix Composites*, 2014, pp. 236-272.
 11. C. J. Armani, M. B. Ruggles-Wrenn, R. S. Hay, G. E. Fair. Creep and microstructure of Nextel™ 720 fiber at elevated temperature in air and in steam, *Acta Materialia* Vol. 61, No. 16, pp. 6114-6124, (2013).
 12. M. Schmücker, F. Flucht, P. Mechnich. Degradation of oxide fibers by thermal overload and environmental effects, *Materials Science and Engineering: A* Vol. 557, pp. 10-16, (2012).
 13. B. Behrens, M. Müller. Technologies for thermal protection systems applied on re-usable launcher, *Acta Astronautica* Vol. 55, No. 3, pp. 529-536, (2004).
 14. D. E. Glass, European directions for hypersonic thermal protection systems and hot structures, *31st Annual Conference on Composites Materials and Structures*, (2007).
 15. I. Boyd, Modeling of plasma formation in rarefied hypersonic entry flows, *45th AIAA Aerospace Sciences Meeting and Exhibit*, 2007, pp. 206.
 16. C. A. Stephens. "Optimization and Fabrication Studies in the Development of Structurally Integrated Thermal Protection System Technology," *NASA ARMD Fundamental Aeronautics Program 2009 Annual Review*. DOI, Atlanta, GA, (2009).
 17. J. T. Dorsey, C. C. Poteet, K. E. Wurster, R. R. Chen. Metallic Thermal Protection System Requirements, Environments, and Integrated Concepts, *Journal of Spacecraft and Rockets* Vol. 41, No. 2, pp. 162-172, (2004).
 18. H. James, A. K. Singh, T. Hyde, R. Andrulonis, M. S. Opliger. Effects of thermal plasma on the microstructure and mechanical behavior of alumina-mullite based oxide/oxide ceramic matrix composites, *Materials Science and Engineering: A* Vol. 886, p. 145711, (2023).